

## FINITE DIFFERENCE SOLUTION OF MIXED BOUNDARY-VALUE ELASTIC PROBLEMS

**S. Reaz Ahmed, Noor Al Quddus and M. Wahhaj Uddin**

Department of Mechanical Engineering, Bangladesh University of Engineering and Technology,  
Dhaka – 1000, Bangladesh

**Abstract** A new numerical method of solution has been developed for the analysis of deformation and stresses in elastic bodies subjected to mixed boundary-conditions. The program is capable of dealing with both regular and irregular shapes of boundaries appropriately. An ideal mathematical model, based on the displacement potential function, has been used in the finite difference solution. The present paper demonstrates the application of the newly developed computational scheme to a widely used body with curved boundaries, namely, involute profile spur gear teeth.

*Keyword: arbitrary-shaped elastic body; displacement potential function; finite-difference technique.*

### INTRODUCTION

The rapid growth in the use of computers in the past decade gave rise to the developments of advanced computational scheme. But somehow the elasticity problems are still suffering from a lot of shortcomings. Actually, the management of boundary conditions and boundary shapes has remained as the biggest hurdle in the solution process of the problems of solid mechanics. The necessity of the management of boundary shape has lead to the invention of the finite element technique with its overwhelming popularity. The other factor of impediment to quality solution of elastic problems is the treatment of the transition in boundary conditions.

The difficulties involved in trying to solve practical stress problems using the existing approaches, for example, the stress function approach [1] and the two displacement functions approach [2], are clearly pointed out in our previous reports [3-6] and also by Durelli [7]. In an attempt to circumvent the difficulties, Dow et al [8] introduced a new boundary modeling approach for the finite difference applications in solid mechanics. They reported that the accuracy of the finite difference method in reproducing the state of stresses along the boundary was much higher than that of finite element method of analysis.

The displacement potential function formulation of two dimensional elastic problems used here was first introduced by Uddin [2]; later Idris [3] used it for obtaining analytical solutions of mixed boundary value elastic problems and Ahmed [4-6] developed the computational scheme to extend its use in obtaining the numerical solutions of a number of mixed boundary value problems. The rationality and reliability of the formulation is checked repeatedly by comparing the

results of mixed boundary value elastic problems obtained through this formulation with those available in the literature. Recently, our work has been extended to include the problems of arbitrary boundary shapes[10]. The present paper demonstrates the application of the newly developed computational scheme to a widely used body with curved boundaries, namely, involute profile spur gear teeth.

### FORMULATION OF THE PROBLEM

With reference to a rectangular co-ordinate system, the differential equations of equilibrium for two-dimensional problems in terms of displacement components are [1]

$$\frac{\partial^2 u}{\partial x^2} + \left(\frac{1-\mu}{2}\right) \frac{\partial^2 u}{\partial y^2} + \left(\frac{1+\mu}{2}\right) \frac{\partial^2 u}{\partial x \partial y} = 0 \quad (1)$$

$$\frac{\partial^2 u}{\partial y^2} + \left(\frac{1-\mu}{2}\right) \frac{\partial^2 u}{\partial x^2} + \left(\frac{1+\mu}{2}\right) \frac{\partial^2 u}{\partial x \partial y} = 0 \quad (2)$$

These two homogeneous elliptic partial-differential equations, with appropriate boundary conditions, have to be solved for the case of a two-dimensional problem when the body forces are assumed to be absent. In the present approach, the problem is reduced to the determination of a single function  $\psi$  [2] instead of finding the two variables  $u$  and  $v$ , simultaneously, satisfying the equilibrium equations (1) and (2). The potential function  $\psi(x,y)$  is defined in terms of displacement components as

$$u = \frac{\partial^2 \psi}{\partial x \partial y}$$

$$v = -\frac{1}{1+\mu} \left[ (1-\mu) \frac{\partial^2 \psi}{\partial y^2} + 2 \frac{\partial^2 \psi}{\partial x^2} \right] \quad (3)$$

When the displacement components in equation (1) and (2) are replaced by  $\psi(x,y)$ , equation (1) becomes an identity and the only condition that has to be satisfied becomes

$$\frac{\partial^4 \psi}{\partial x^4} + 2 \frac{\partial^4 \psi}{\partial x^2 \partial y^2} + \frac{\partial^4 \psi}{\partial y^4} = 0 \quad (4)$$

Therefore, the problem is formulated in such a way that a single function  $\psi$  has to be evaluated from the bi-harmonic equation (4), satisfying the conditions that are specified at the boundary. Now, the boundary conditions, at any point on an arbitrary-shaped boundary, are known in terms of the normal and tangential components of displacement,  $u_n$  and  $u_t$ , and of stresses,  $\sigma_n$  and  $\sigma_t$ . These four components are first expressed in terms of  $u$ ,  $v$ ,  $\sigma_x$ ,  $\sigma_y$ ,  $\sigma_{xy}$  [6]—the components of displacements and stress with respect to the reference axes  $x$  and  $y$  and finally, in terms of the function  $\psi$ , as follows:

$$u_n(x, y) = -\frac{2m}{1+\mu} \frac{\partial^2 \psi}{\partial x^2} - \frac{m(1-\mu)}{1+\mu} \frac{\partial^2 \psi}{\partial y^2} + l \frac{\partial^2 \psi}{\partial x \partial y} \quad (5)$$

$$u_t(x, y) = -\frac{2l}{1+\mu} \frac{\partial^2 \psi}{\partial x^2} - \frac{l(1-\mu)}{1+\mu} \frac{\partial^2 \psi}{\partial y^2} - m \frac{\partial^2 \psi}{\partial x \partial y} \quad (6)$$

$$\sigma_n(x, y) = \frac{E}{(1+\mu)^2} \left[ -2lm \frac{\partial^3 \psi}{\partial x^3} + (l^2 - 2m^2 - \mu m^2) \frac{\partial^3 \psi}{\partial x^2 \partial y} + 2lm\mu \frac{\partial^3 \psi}{\partial x \partial y^2} - (\mu l^2 + m^2) \frac{\partial^3 \psi}{\partial y^3} \right] \quad (7)$$

$$\sigma_t(x, y) = \frac{E}{(1+\mu)^2} \left[ -(l^2 - m^2) \frac{\partial^3 \psi}{\partial x^3} - lm(\mu + 3) \frac{\partial^3 \psi}{\partial x^2 \partial y} + \mu(l^2 - m^2) \frac{\partial^3 \psi}{\partial x \partial y^2} + lm(\mu - 1) \frac{\partial^3 \psi}{\partial y^3} \right] \quad (8)$$

The computational work in solving any problem remains the same in the present case as it was in the case of  $\phi$ -formulation, since both of them have to satisfy the same bi-harmonic equation. But the  $\psi$ -formulation is free from the inability of the  $\phi$ -formulation in handling the mixed boundary condition.

### SOLUTION PROCEDURE

Finite-difference technique is used to discretize the governing bi-harmonic equation and also the differential equations associated with the boundary conditions. The discrete values of  $\psi(x,y)$  at the mesh points of the domain concerned (see Fig. 1), is solved from the system of linear algebraic equations resulting from the discretization of the governing equation and the associated boundary conditions.

The present scheme involves evaluation of the function  $\psi$  at the nodal points of rectangular grids over a geometrically irregular region, where the boundary may not always pass through the rectangular mesh points, as shown in Fig.1. The governing bi-harmonic equation, which is used to evaluate the function  $\psi$  only

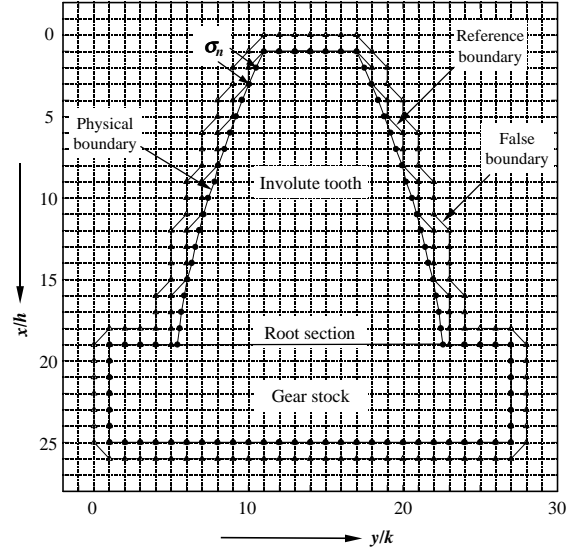


**Fig.1 Discretization scheme for the gear tooth domain.** ( $m_0 = 10$  mm,  $a = m_0$ ,  $b = 1.25 m_0$ ,  $\theta_p = 20^\circ$ ,  $d_p = 500$  mm, load  $\sigma_n/E = -3e-4$ ).

at the internal mesh points, is expressed in its corresponding difference equation using central difference operators. The complete finite-difference expression of the bi-harmonic equation (4) is given by

$$R^4 \{ \psi(i-2, j) + \psi(i+2, j) \} - 4R^2 (1+R^2) \{ \psi(i-1, j) + \psi(i+1, j) \} - 4(1+R^2) \{ \psi(i, j+1) + \psi(i, j-1) \} + (6R^4 + 8R^2 + 6) \psi(i, j) + 2R^2 \{ \psi(i-1, j-1) + \psi(i-1, j+1) + \psi(i+1, j-1) + \psi(i+1, j+1) \} + \psi(i, j-2) + \psi(i, j+2) = 0 \quad (9)$$

The corresponding grid structure of the governing equation for an arbitrary internal mesh point  $(i, j)$  is shown in Figure 2. It is thus clear that when the point of application  $(i, j)$  becomes an immediate neighbour of the physical boundary, the equation will involve mesh points both interior and exterior to the physical boundary.

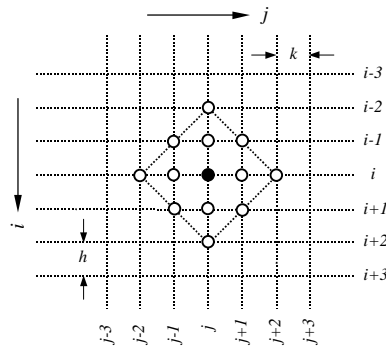


**Fig.2 Grid structure for the governing bi-harmonic equation.**

An imaginary (false) boundary, exterior to the reference boundary of the domain is introduced as shown in the Fig.1. As the differential equations associated with the boundary conditions contain second-

and third-order derivatives of the function  $\psi$ , the use of central difference expressions ultimately leads to the inclusion of points exterior to the false boundary. The derivatives in the expressions of boundary-conditions are thus replaced by their backward- or forward-difference formulae, keeping the order of the local truncation error the same.

Any boundary-value at a boundary-point, not matching with the field grid points, is replaced by the linear interpolation of its value at the two or four neighbouring grid points, one of which is designated as the reference point, which is unique to the boundary point.

The difference equations of the boundary conditions for any arbitrary point on the boundary, not matching with the field grid points, can readily be obtained by knowing the actual position of the boundary point with respect to its reference grid point. Referring to Fig. 3, the difference expressions for boundary conditions at any arbitrary point P, the location of which is defined by

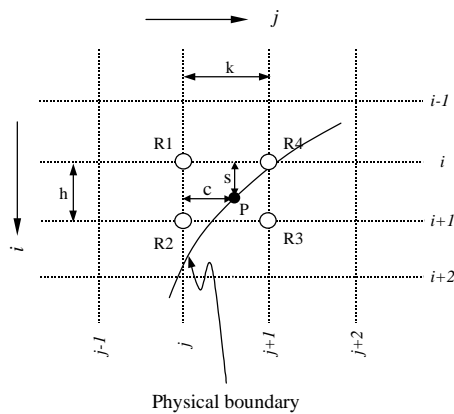


Fig. 3 Locators 'c' and 's' of the boundary point P with respect to its reference point R1.

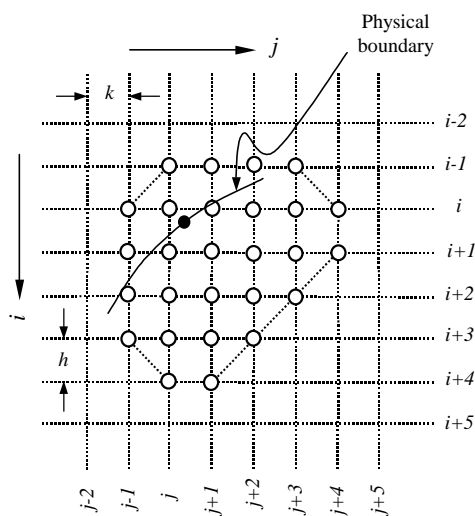


Fig. 4 Grid structure for  $\sigma_n$  or  $\sigma_t$  at top-left boundary (boundary point not matching with field grid point)

c and s, is obtained by using linear interpolation of the expressions of the boundary-values at the points R1, R2, R3 and R4. The final form of the grid structure so obtained for the stress components for boundary points not matching with the field grid points is illustrated in Fig.4.

Since there are two conditions to be satisfied at an arbitrary point on the physical boundary of the elastic body, two difference equations are assigned to a single point on the boundary. Out of these two equations, one is used to evaluate the function  $\psi$  at the reference point corresponding to the physical boundary point and the remaining one for the corresponding point on the false boundary. The discrete values of the potential function,  $\psi(x,y)$ , at mesh points are solved from the system of algebraic equations resulting from the discretization of the governing equation and the associated boundary conditions, by the use of direct method of solution (Choleskey's triangular decomposition method). Finally, the same difference equations are organized for the evaluation of all the parameters of interest in the solution of the body at every interior as well as boundary points from the  $\psi$  values at mesh points of the domain.

## RESULTS AND DISCUSSIONS

Gear tooth has been taken as the arbitrary-shaped elastic body, made of ordinary steel ( $\mu=0.3$ ,  $E=209$  GPa), to obtain the numerical values of stresses in it as well as the deformed shape of it under load.

The conjugate loading on the tooth is approximated here by the distribution of normal load over a small region at the contact point. It should be mentioned here that, because of the Saint-Venant's principle, the distribution of loading at the contact point does not affect the stresses in the gear at the critical region of the fillets or at any other critical section of the tooth, far away from the loading, so long the total loading remains the same. Obviously, the stresses at and near the contact point is very much dependent on the approximation in the assumed distribution of loading at the contact point.

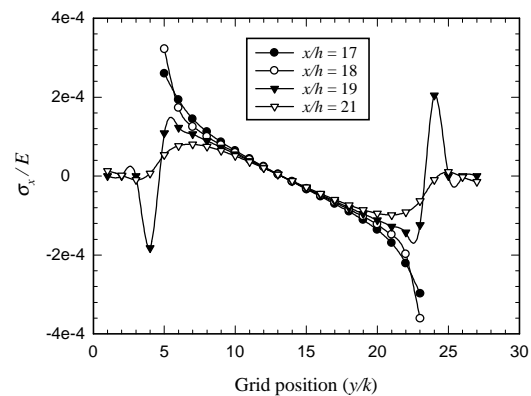


Fig. 5 Radial stresses ( $\sigma_r/E$ ) at sections  $x/h = 17, 18, 19$  and 21 of the gear tooth

The stresses at different sections of the tip-loaded spur gear tooth, shown in Fig.1 (referred to as type-A here), are presented in Figs 5-6. Overall, the magnitudes of the stresses  $\sigma_y$  and  $\sigma_{xy}$  are smaller than that of the radial stress  $\sigma_x$ . Maximum stresses are found to occur around the root section of the tooth, and the fillet zone is the most critical section in terms of stresses. The magnitude of stresses just below the root section is lower and gradually decreases towards the center of the gear but does not become zero on the bottom boundary, which is considered rigidly fixed. The load applied normally to the tooth face near the tip has basically two components, one of bending, which is compressing the load-free side and tensioning the loaded side of the tooth, while the other is compressing over the whole section. Thus, the combined effect of bending and compression gives lower value of tension in the load-side fillet and higher value of compression in the load free-side fillet (Fig.5).

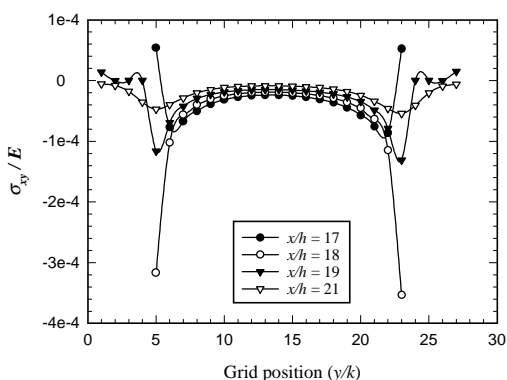


Fig. 6 Shearing stresses ( $\sigma_{xy}/E$ ) at sections  $x/h = 17, 18, 19$  and  $21$  of the gear tooth

The deformed tooth profile of the gear with respect to its initial undeformed profile under the loading at different regions are illustrated in Fig.7. The profiles show that maximum displacement occurs under the tip loading. The tooth deflects in the direction of load and the deflection is maximum at the tip and gradually decreases towards the root.

Another spur gear tooth (profile: involute,  $m_0 = 10$  mm,  $\theta_p = 20^\circ$ ,  $a = m_0$ ,  $b = 1.157 m_p$ ,  $d_p = 200$  mm) is considered here for comparing the present  $\psi$ -solution

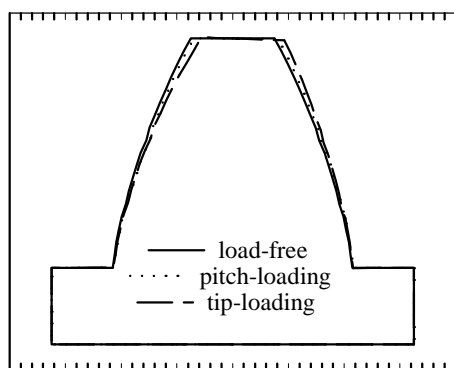


Fig.7 Tooth profiles under root loading (displacements are 100 times enlarged)

with the published FEM results[9]. The values of radial stress at the root section, due to the tip, pitch and root loading are presented in Table-1 along with the FEM results. The magnitudes of the stresses at the extreme end of the root section, especially at the tension side, are found to be in good agreement. However, the FEM solution [5] predicts lower value of the compressive stress at the bottom surface of the root section than that

Table –1 Comparison of present solution for stresses with that of FEM solution

Load	Radial stress at the Root section (MPa)			
	Loaded surface		Load-free surface	
	FDM	FEM	FDM	FEM
Tip	108.45	110.00	-123.90	-127.00
Pitch	68.87	71.00	-78.13	-100.00
Root	49.14	55.00	-38.09	-48.00

at points above it. This is highly unlikely, as the bending stress is the highest at the bottom, which is further enhanced due to the effect of stress concentration at that point.

In our present approach, a single variable is evaluated at each point instead of solving for two variables simultaneously as in the case of FEM, which reduces our computational work drastically. It is noted that the time taken to solve a gear tooth (29 X 27 mesh) on a personal computer (450 MHz) was found to be 3.91 s. The accuracy as well as the reliability of the present method has been verified repeatedly by comparing the results with available solutions [4,10].

### CONCLUSIONS

The difficulties of managing the boundary shapes in finite difference techniques of analysis for which the finite-element method of solution of elastic problems was invented with a manifold increase of computational works and a lot of loss of sophistication is overcome here by a novel computational technique in the management of boundary shapes in the finite-difference method of solution. Both the qualitative and quantitative results of the spur gear tooth, and their comparison with those of FEM solution establish the reliability and suitability of the present numerical model.

### NOMENCLATURE

- E elastic modulus of the material
- $\mu$  Poisson's ratio
- $u, v$  displacement components in the x- and y-directions
- $\sigma_x, \sigma_y$  normal stress components in the x- and y-directions
- $\phi$  Airy's stress function

$\psi$	displacement potential function
$u_n, u_t$	normal and tangential components of displacement on the boundary
$\sigma_n, \sigma_t$	normal and tangential components of stress on the boundary
$l, m$	direction cosines of the normal at any point on the boundary
$h, k$	mesh lengths in the x- and y- directions
$R$	$k/h$
$a, b$	addendum and dedendum of the gear
$m_o, d_p, \theta_p$	module, pitch diameter, pressure angle of gear tooth
$c, s$	locators in y- and x- directions, with respect to the reference grid point

shaped elastic bodies", *Advances in Engineering Software*, Vol. 31, No. 3 (2000), pp. 173-184.

### REFERENCES

1. Timoshenko S, Goodier JN. *Theory of Elasticity*. (3<sup>rd</sup> edn.). McGraw-Hill, New York, N. Y. (1979).
2. Uddin, M.W., "Finite Difference Solution of Two-Dimensional Elastic Problems with Mixed Boundary Conditions", M. Sc. Thesis, Carleton University, Canada, (1966).
3. Idris, A.B.M., Ahmed, S.R. and Uddin, M.W., "Analytical Solution of a 2-D Elastic Problem with Mixed Boundary Conditions", *Journal of the Institution of Engineers (Singapore)*, Vol. 36, No. 6 (1996), pp. 11-17.
4. Ahmed, S.R., Khan, M.R., Islam, K.M.S. and Uddin, M.W., "Analysis of Stresses in Deep Beams Using Displacement Potential Function" *Journal of Institution of Engineers (India)*, Vol. 77, (1996), pp. 141-147.
5. Ahmed, S.R., Idris, A.B.M. and Uddin, M.W., "Numerical Solution of Both Ends Fixed Deep Beams", *Computers & Structures*, Vol. 61, No. 1 (1996), pp. 21-29.
6. Ahmed, S.R., Khan, M.R., Islam, K.M.S., and Uddin, M.W., "Investigation of stresses at the fixed end of deep cantilever beams", *Computers & Structures*, Vol. 69, (1998), pp. 329-338.
7. Durelli, A.J. and Ranganayakamma, B., "Parametric solution of stresses in beams", *Journal of Engineering Mechanics*, Vol. 115, No. 2 (1989), pp. 401-415.
8. Dow, J.O., Jones, M.S. and Harwood, S.A., "A new approach to boundary modeling for finite difference applications in solid mechanics", *International Journal for Numerical Methods in Engineering*, Vol. 30, (1990), pp. 99-113.
9. Ramamurti, V. & Rao, M.A., "Dynamic Analysis of Spur Gear Teeth", *Computers and Structures*, Vol. 29, No. 5, (1988), pp. 831-843.
10. Akanda, M.A.S., Ahmed, S.R., Khan, M.R., and Uddin, M.W., "A finite-difference scheme for mixed boundary-value problems of arbitrary-